Current Biology, Vol. 15, 886–893, May 24, 2005, ©2005 Elsevier Ltd All rights reserved. DOI 10.1016/j.cub.2005.03.051

A GABAergic Mechanism Is Necessary for Coupling Dissociable Ventral and Dorsal Regional Oscillators within the Circadian Clock

Henk Albus,[1,2] Mariska J. Vansteensel,[1] Stephan Michel,[1] Gene D. Block,[2] and Johanna H. Meijer[1,*]
[1]Department of Neurophysiology
Leiden University Medical Center
Wassenaarseweg 62
Post Office Box 9604
2300 RC Leiden
The Netherlands
[2]Center for Biological Timing and Department of Biology
University of Virginia
Charlottesville, Virginia 22903-2477

Summary

Background: Circadian rhythms in mammalian behavior, physiology, and biochemistry are controlled by the central clock of the suprachiasmatic nucleus (SCN). The clock is synchronized to environmental light-dark cycles via the retino-hypothalamic tract, which terminates predominantly in the ventral SCN of the rat. In order to understand synchronization of the clock to the external light-dark cycle, we performed ex vivo recordings of spontaneous impulse activity in SCN slices of the rat.
Results: We observed bimodal patterns of spontaneous impulse activity in the dorsal and ventral SCN after a 6 hr delay of the light schedule. Bisection of the SCN slice revealed a separate fast-resetting oscillator in the ventral SCN and a distinct slow-resetting oscillator in the dorsal SCN. Continuous application of the $GABA_A$ antagonist bicuculline yielded similar results as cut slices. Short application of bicuculline at different phases of the circadian cycle increased the electrical discharge rate in the ventral SCN but, unexpectedly, decreased activity in the dorsal SCN.
Conclusions: GABA transmits phase information between the ventral and dorsal SCN oscillators. GABA can act excitatory in the dorsal SCN and inhibits neurons in the ventral SCN. We hypothesize that this difference results in asymmetrical interregional coupling within the SCN, with a stronger phase-shifting effect of the ventral on the dorsal SCN than vice versa. A model is proposed that focuses on this asymmetry and on the role of GABA in phase regulation.

Introduction

The suprachiasmatic nucleus (SCN) contains a circadian pacemaker that is synchronized to the environmental light-dark cycle [1]. Circadian rhythmicity is generated by a molecular feedback loop that involves several identified clock genes and their protein products [2]. The cell-autonomous nature of rhythm generation results in the presence within the SCN of multiple neuronal oscillators that exhibit circadian rhythms in clock-gene expression and electrical-impulse frequency [3, 4]. The composite waveform of these independent but coupled neuronal oscillators provides a reliable and precise representation of the day-night cycle at the SCN tissue level [5–7].

For circadian pacemakers to perform useful work, they must be set to local time. This occurs through the process of synchronization, or "entrainment," which involves specialized photoreceptors and pathways [8, 9]. Phase-shifting studies have been helpful in studying the underlying pacemaker organization. For example, the multioscillator composition of the *Drosophila* circadian system was discovered during readjustments to phase-advancing light pulses [10]. In mammals, phase-shifting protocols have led to the observation of transient desynchronization among molecular rhythms [11] and between molecular and electrical rhythms [12] and of regional differences in the speed of resetting within the SCN [13].

It is well established that the SCN is a heterogeneous structure. An important distinction between ventral and dorsal SCN compartments of the rat was originally based on functional anatomical evidence [14, 15] and was confirmed by differences in immediate early-gene and clock-gene expression within the SCN [16–18]. The ventrolateral (or core) SCN contains cells expressing vasoactive intestinal peptide (VIP) or gastrin releasing peptide (GRP). They receive direct excitatory retinal input from melanopsin-containing ganglion cells that use glutamate and pituitary adenylyl cyclase-activating peptide (PACAP) as transmitter and neuromodulator [19]. Ventral SCN neurons project to dorsomedial (also called shell)-region cells that typically express vasopressin (VP) and receive only sparse retinal innervation [20]. Evidence for independent oscillators in these SCN regions emerged from studies monitoring VIP- and VP-release in cultured organotypic slices [21, 22] and long-term measurements of *Per1* with a luciferase reporter [4]. Functional differences between the dorsal and ventral SCN were recently demonstrated when molecular oscillations were forced into desynchrony by exposing rats to short light-dark cycles [23].

These findings raise questions about the mechanisms by which the ventral and dorsal SCN eventually synchronize to function as a clock with a coherent timing signal. To address this issue, we performed real-time electrical-activity recordings simultaneously in the ventral and dorsal parts of coronal SCN slices after a shift in the light-dark cycle. On the first and third day after a delay, we observed bimodal patterns (i.e., two components) of electrical activity in dorsal and ventral SCN, with one shifted and one unshifted component. These components resynchronized, resulting in a completely phase-shifted, unimodal rhythm in electrical activity on day 6 after the shift of the light cycle. Surgical isolation as well as application of the $GABA_A$ receptor antagonist bicuculline prevented the interplay between dorsal and ventral SCN and revealed local phase-resetting behavior of the two areas. The results lead us to

*Correspondence: j.h.meijer@lumc.nl

suggest that the ventral SCN is directly reset by light, and the dorsal SCN is indirectly reset through excitatory GABAergic pathways. Importantly, the electrical output of clock neurons reflects both intrinsic rhythmicity and rhythmicity imposed from other SCN neurons.

Results

Intact Slices

Electrical-activity recordings were performed in acutely prepared brain slices at the end of a 6 hr delayed light-dark cycle or on day 3 or 6 in constant darkness after the delay (see Figure S1A in the Supplemental Data available with this article online). The recordings were performed simultaneously in the ventral and dorsal SCN by two stationary electrodes. Immediately after the shift in the light schedule, two components in SCN electrical activity appeared in 67% (10 of 15) of the recordings in both the ventral and dorsal SCN (Figure 1B; Figure S2). The bimodal patterns showed very similar peak times in the two regions. As compared to unshifted control slices (mean peak at Zeitgeber time [ZT] 6.1 ± 0.7; Figure 1A; Figure S1A), the peak time of the first component of the bimodal pattern was delayed completely ($\Delta\phi$ = –6.2 ± 0.6 hr, n = 10, $p < 0.001$), whereas the second component was not significantly shifted ($\Delta\phi$ = –1.8 ± 0.6 hr, n = 10, $p > 0.1$). The peak times of the two components were significantly different ($p < 0.001$). The occurrence of bimodal peaks in the electrical-activity rhythms of the ventral and dorsal SCN decreased to 42% (5 of 12 recordings) on day 3 in constant darkness ($\Delta\phi$ = –7.9 ± 0.8 hr, n = 5, $p < 0.001$ and $\Delta\phi$ = –2.8 ± 0.8 hr, n = 5, $p < 0.05$; peak times were also significantly different from one another, $p < 0.01$; Figure 1C). When unimodal peaks were obtained on days 1 and 3 after the delay in the light schedule, intermediate phase shifts of –3.6 ± 0.7 hr (n = 5, $p < 0.01$) and –3.5 ± 0.7 hr (n = 7, $p < 0.01$) were observed, respectively. All recordings on day 6 in constant darkness showed a unimodal rhythm that was fully shifted ($\Delta\phi$ = –6.0 ± 0.7 hr, n = 12, $p < 0.001$; Figure 1D).

The widths of the neuronal-activity peaks were calculated with the half-maximum values of increasing and decreasing slopes. On the first day after the shift, the peak widths were not significantly different from the peak widths before the delay of the light-dark cycle ($p > 0.05$). The peak widths that were measured on day 3 or 6 in darkness were significantly smaller ($p < 0.05$). Comparison of the peak widths with the activity time (α) of rat behavioral activity rhythms revealed a strong correlation (R = –0.99, $p < 0.05$), indicating functional significance for both components in regulating behavioral activity, consistent with de la Iglesia et al. [23] (Supplemental Results; Figures S3 and S4).

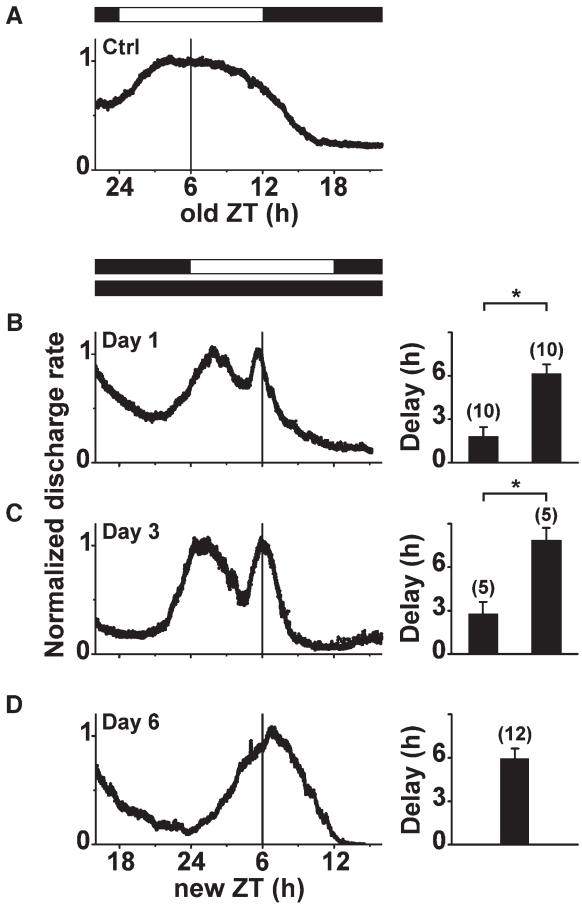

Figure 1. Recordings of SCN Electrical Activity In Vitro before and after a 6 hr Phase Delay of the Light-Dark Regime

(A) The electrical-activity rhythm of control (Ctrl) slices from animals not exposed to a shift in light-dark cycle showed unimodal peaks at old ZT 6.

(B and C) Bimodal peaks emerged on the first and third day after the delay, both in the ventral and dorsal SCN, with one incompletely shifted and one completely shifted (new ZT 6) component.

(D) On day 6 after the shift, exclusively unimodal peaks were observed that were shifted completely.

The electrical-activity traces are individual examples of neuronal ensemble recordings. Horizontal bars indicate the light-dark cycle and old and new ZT is indicated on the x axis. For reference, ZT 6 is indicated by a vertical line. The electrical activity is counted per 10 s and is presented on a normalized scale. The histograms represent average (± the standard error) phase delays of the peak times of the unshifted and shifted components for days 1 and 3, with numbers of recordings indicated above the bars. The bars on the left represent data from the first components, and the bars on the right refer to the fully shifted component (asterisks: $p < 0.01$). On day 6, unimodal peaks were obtained in 100% of the recordings. The histogram indicates the average phase delay.

Cut Slices

The SCN was cut horizontally, separating the slice into dorsal and ventral sections, to investigate the contribution of different regions to the bimodal-activity patterns. Recordings in the ventral part of the SCN revealed the presence of a unimodal electrical-activity component that was phase delayed by 4 hr ($\Delta\phi$ = –4.1 ± 0.6 hr, n = 11, $p < 0.001$; Figures 2A–2C). Recordings in the dorsal part of the cut SCN revealed the presence of a unimodal component that was unshifted ($\Delta\phi$ = –0.6 ± 0.7 hr, n = 7, $p > 0.5$). The peak times of the components in the dorsal and ventral SCN were significantly different ($p < 0.001$), and also, the times of the troughs of the electrical-activity rhythm and of the half-maximum value differed significantly between dorsal and ventral SCN ($p < 0.01$). The absolute discharge rate in the ven-

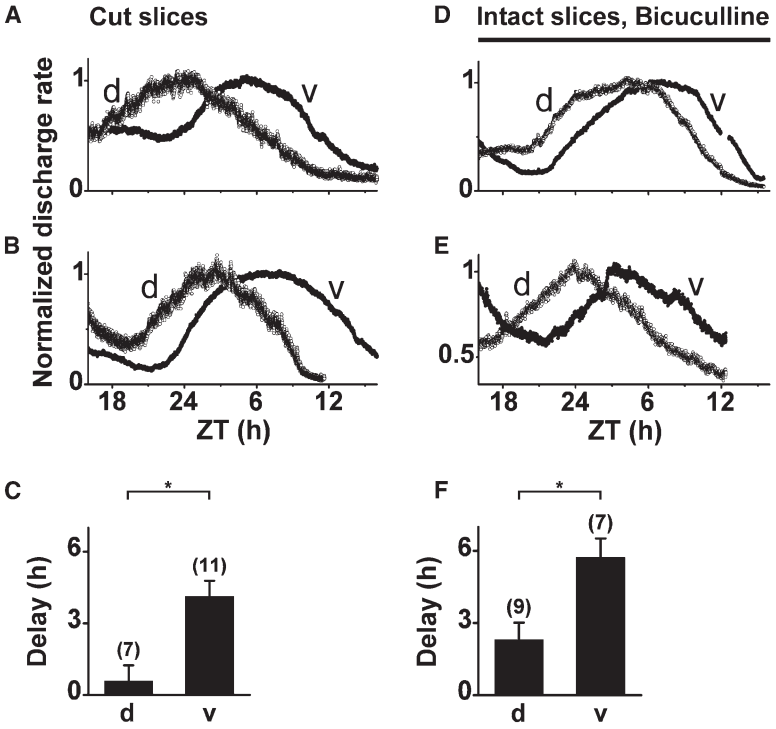

Figure 2. Bisection and Continuous Bicuculline Application Reveal Local Phase-Resetting Behavior of the Ventral and Dorsal SCN

(A and B) Two examples from recordings on the first day after a 6 hr phase delay in the dorsal (d) and ventral (v) parts of the SCN when they are separated by a cut. The results show unimodal electrical-activity rhythms in the dorsal and ventral SCN, which were out of phase. Discharge rate is plotted per 10 s on a normalized scale. ZT of the delayed light-dark regime is indicated on the x axis.

(C) Mean (± the standard error) phase delays of the unimodal peaks obtained in the dorsal (d) and ventral (v) parts of a cut SCN. The unimodal peak obtained in the ventral SCN shows a large phase shift, whereas the peaks recorded in the dorsal SCN are not significantly shifted. The number of recordings is indicated above the bars (asterisk: $p < 0.001$).

(D and E) Examples of simultaneous recordings within one slice on the first day after a 6 hr phase delay in the dorsal (d) and ventral (v) intact SCN in the continuous presence of 20 μM bicuculline. Similar to a cut, the presence of a $GABA_A$ receptor blocker resulted in unimodal peaks in the dorsal and ventral SCN, which were out of phase. A black bar at the top indicates the timing of the bicuculline application. Axes as in (A) and (B).

(F) Average (± the standard error) phase delays of the peak times obtained in the dorsal (d) and ventral (v) SCN (asterisk: $p < 0.01$). Above each bar, the number of recordings contributing to the average is indicated. The peak of the dorsal SCN activity was only slightly phase shifted, but the peak of the ventral SCN activity was completely delayed. The phase difference between the rhythms recorded from the dorsal and ventral SCN indicates that signals from one part of the SCN are not directly measured by an electrode that is placed in the other part of the SCN.

tral SCN was higher than in the dorsal SCN (ventral peak: 235 ± 51 Hz; dorsal peak: 69 ± 11 Hz), but the peak widths did not differ ($p > 0.8$).

In a few cases, the slices were cut in such a way that the dorsal part contained about two-thirds of the dorsal-ventral extension of the SCN. Recordings in the larger dorsal parts revealed bimodal peaks with a very small secondary component in 57% of the cases (4 of 7), consistent with the notion that some rapidly shifting neurons of the ventral SCN region were now included in the dorsal part of the preparation (Figure S5).

In two additional series of experiments, we recorded in cut slices from animals subjected to a 6 hr advance of the light-dark cycle or from control animals experiencing no shift. After advances, we found a large phase shift in the ventral SCN and a small shift of the dorsal part. Slices from control animals showed no phase difference between the dorsal and ventral peak times (see Supplemental Results and Figures S1B, S1C, and S6).

Bicuculline Experiments

Long-Term Blockade of GABAergic Activity

To investigate the role of γ-aminobutyric acid (GABA) in communication between ventral and dorsal SCN, we applied the $GABA_A$ receptor blocker bicuculline to intact slices. Brain slices were prepared at the end of the 6 hr phase-delayed light-dark cycle at ZT 12. Bicuculline (20 μM) administration started several hours after slice preparation (between ZT 14.6 and 15.4) and lasted for at least 20 hr to cover the period with elevated electrical activity. The application of bicuculline significantly reduced the occurrence of bimodal electrical-activity patterns (chi-square test, $p < 0.05$). Instead, unimodal electrical-activity rhythms were obtained in most recordings (73%, 16 of 22). The unimodal rhythms that were recorded in the ventral SCN were completely delayed ($\Delta\phi = -5.7 \pm 0.8$ hr, $n = 7$, $p < 0.001$; Figures 2D–2F). In the dorsal SCN, rhythms were delayed by −2.3 ± 0.7 hr ($n = 9$, $p < 0.05$). The peak times of the electrical-activity rhythms in the dorsal and ventral SCN were significantly different from each other ($p < 0.01$), as well as the troughs and the half-maximum values ($p < 0.05$). The obtained peak times in the presence of bicuculline did not significantly differ from the times recorded in the cut SCN after a 6 hr delay in the light-dark cycle (independent t tests, $p > 0.05$). Moreover, they did not differ significantly from the first and second components of the bimodal peaks obtained in intact slices without bicuculline (independent t tests, $p > 0.05$). Chronic application of bicuculline did not significantly change the peak width of the unimodal pattern obtained from the ventral or dorsal SCN in comparison to data from the dorsal and ventral parts of cut slices (independent t tests, $p > 0.05$).

Temporal and Spatial Differences in GABA Responsiveness

Bicuculline pulses (20 μM, 30 min in duration) were applied to intact slices to investigate the effects of endog-

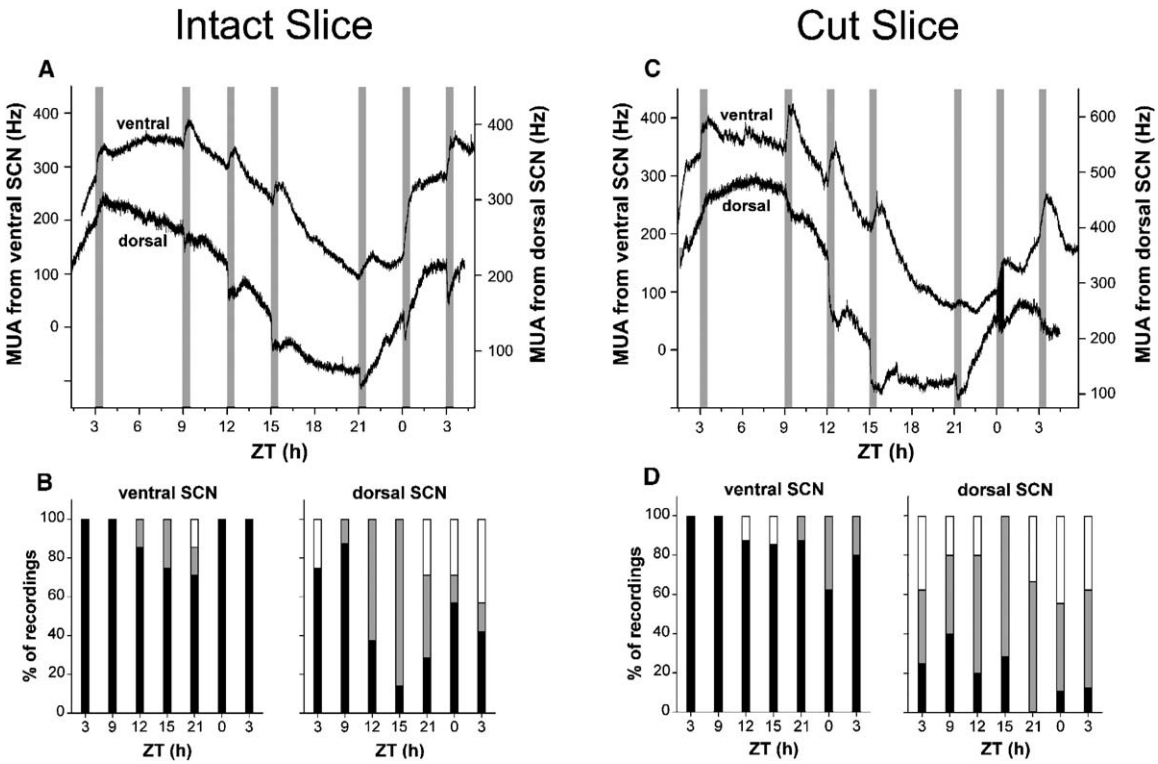

Figure 3. Pulsed Bicuculline Application

(A and C) Examples of responses recorded simultaneously in the dorsal and ventral SCN of intact (A) or cut (C) slices to 30 min bath application of bicuculline. Note the predominantly excitatory effects of bicuculline in the ventral SCN, as opposed to the mainly inhibitory effects in the dorsal SCN. ZT is indicated on the x axis, and frequency of multiunit activity in the ventral and dorsal SCN are indicated on the left and right sides of the graphs, respectively. Gray bars indicate the times of bicuculline application.

(B and D) Distribution of response types in the ventral and dorsal SCN of intact (B) or cut (D) slices during bicuculline application. Bars indicate the percentages of responses with a significant excitation (black), a significant inhibition (gray), or no change in neuronal activity (white) at the different ZT time points.

enous GABA in the dorsal and ventral SCN. Pulses were given at ZT 3, 9, 12, 15, 21, and 0. The average change in electrical discharge of the dorsal SCN in response to bicuculline pulses (n = 50) was significantly different from that of the ventral SCN (n = 52, $p < 0.001$). The ventral SCN exhibited predominantly excitatory responses to bicuculline, as expected from a GABAergic receptor blocker (Figures 3A and 3B), with a mean increase in electrical activity of 23% ± 2% (n = 45). The dorsal SCN responded in an excitatory fashion during early- and midday. During the end of the day and beginning of the night, however, we predominantly observed inhibitory responses to bicuculline in the dorsal SCN, with an average decrease of electrical activity of 14% ± 2% (n = 18). The maximum number of inhibitory responses was observed at ZT 15 (86%, 6 of 7). This was significantly different from the number of inhibitory responses in the ventral SCN at that time (25%, 2 of 8, chi-square test, $p < 0.05$).

GABA Responsiveness in Separated Ventral and Dorsal SCN

Pulsed bicuculline experiments were repeated in cut slices in order to narrow the site of action of bicuculline to the respective SCN area (Figures 3C and 3D). We observed a difference in the average response of dorsal (n = 61) and ventral SCN (n = 51, $p < 0.001$). In addition, we found a clear difference in the sign of the responses between dorsal and ventral SCN. The ventral SCN showed mainly excitatory responses to bicuculline (Figure 3D), with an average increase in neural activity of 19% ± 2% (n = 44). The dorsal SCN showed almost no excitatory responses to the $GABA_A$ blocker. Throughout the cycle, a mean decrease in discharge rate of 14% ± 1% (n = 30) was obtained. These data indicate an excitatory action of endogenous GABA in the dorsal SCN.

Discussion

In the present experiments, bimodal patterns in electrical-activity rhythms were found in SCN slices from rats subjected to a 6 hr phase delay in the light-dark cycle. These bimodal patterns were similar in the ventral and dorsal SCN, with no differences in peak times observed between the two recording sites. On the first day after the delay of the light cycle, one component of the bimodal rhythms was not shifted, whereas the other was completely delayed. Over several days in constant darkness, the components resynchronized, resulting in a unimodal, completely delayed rhythm.

After surgical separation of the dorsal and ventral portions of the SCN, unimodal electrical-activity rhythms were observed in both areas of the SCN. The two rhythms were out of phase, with peaks in the dorsal and ventral regions corresponding with the two components in intact slices. The data show that the ventral and dorsal parts of the SCN contain oscillators that reset with different kinetics and that both oscillators drive a rhythm in electrical-impulse frequency. For both delays and advances, the ventral SCN appears to shift rapidly, whereas the dorsal SCN requires more days to shift. Importantly, the absence of a secondary peak in cut slices indicates that electrical activity is normally transmitted from dorsal to ventral SCN and vice versa. The transmission of electrical signals results in very similar bimodal electrical-activity patterns in the dorsal and ventral SCN in intact slices during resetting of the clock. Under steady-state conditions, however, the two SCN areas are synchronized, resulting in a unimodal activity pattern. This is different from the bimodal pattern that was observed in steady-state conditions in horizontal-slice preparations of the hamster SCN ([24], but see [25]).

In situ hybridization studies have shown dissociation between rhythms in clock-gene expression in the ventral and dorsal SCN in response to a delaying shift of the light-dark cycle. Oscillations in *rPer1*, *rPer2*, *rCry1*, and rCRY1 in the ventrolateral SCN phase shifted more quickly than in the dorsomedial SCN [13]. Our findings indicate that the temporal complexity observed in molecular expression is also reflected in electrical-impulse frequency of SCN neurons, including an overshoot in phase shift in the ventral SCN. However, the spatial distribution of the signal is substantially different. Whereas molecular expression profiles show regional differences within the intact SCN, for electrical activity, these differences became apparent only in cut slices. Taken together, the data indicate that in the ventral as well as dorsal SCN, one of the electrical-activity components is endogenously driven by the molecular clock, whereas the other component is driven by neuronal transmission of electrical-impulse activity from the other part of the SCN. As a consequence, the endogenous peak remains after a cut, whereas the imposed peak in the same region disappears. Importantly, our studies reveal that electrical activity integrates phase information from endogenous oscillations within different regions of the SCN (Figure 4A).

Although our analysis focused on phase differences between regions of the SCN, there is also evidence that within a region, individual cells display phase differences [4–6]. Consequently, our recordings within a region represent the composite waveform of many oscillators that are slightly out of phase. Several factors, such as Na^+-dependent action potentials [4, 26], GAP junctions [27–29], GABA [30, 31], or other transmitters or factors have been proposed to possibly play a role in synchronization among SCN neurons (for review, see [32]). It is probable that electrical coupling is used for short distances within one region of the SCN [23, 29] and that chemical transmitters, such as GABA, are used for interregional coupling. We used the $GABA_A$ receptor blocker bicuculline because of the prevalence of $GABA_A$ receptors in the SCN [33, 34] and its lack of

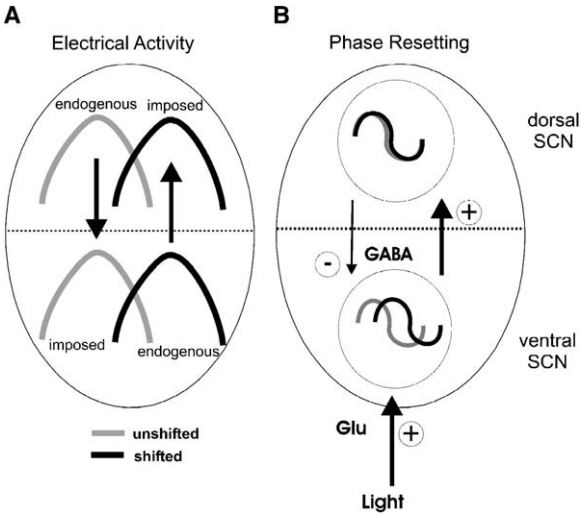

Figure 4. Regulation of Electrical Activity in Dorsal and Ventral SCN

(A) Transmission of electrical activity from one side of the SCN to the other. In both dorsal and ventral intact SCN, bimodal patterns in electrical activity were observed after a delay in the light-dark cycle with a shifted (black) and unshifted (gray) component. When the ventral and dorsal parts were separated by a cut, we observed that the shifted component remained in the ventral SCN, whereas in the dorsal part, the unshifted component remained. We conclude that the secondary electrical-activity peaks, which could be observed in intact slices only, were imposed by electrical activity that was transmitted from the other side of the SCN (arrows). The data indicate that the SCN integrates electrical information from different SCN regions.

(B) Light entrainment of the SCN. Light information is transduced from the retina to the retinorecipient ventral part of the SCN via the retinohypothalamic tract (RHT) and depends on glutamatergic neurotransmission. Our results indicate that the ventral SCN responds rapidly to a shift in the light cycle, whereas the dorsal part of the SCN requires several days to resynchronize. We propose that the ventral SCN has a strong phase-shifting effect on the dorsal part (thick arrow). The dorsal SCN, in contrast, seems to have a weak phase-shifting effect on the ventral part (thin arrow). Because we observed complete uncoupling of the two parts under bicuculline, our data indicate an important role for GABA in synchronization of the ventral and dorsal SCN. The excitatory effect of GABA on the dorsal SCN (+) and the inhibitory effect on the ventral SCN (–) may account for the asymmetry in coupling between dorsal and ventral SCN.

phase-shifting effects [35–38]. We hypothesized that a role for GABA in coupling would become evident by an attenuation of the secondary activity peak under bicuculline conditions. Application of low concentrations of bicuculline (20 μM) resulted in a strong reduction in the incidence of bimodal peaks. Instead, unimodal out-of-phase electrical-activity peaks were observed in the ventral and dorsal SCN. In fact, the results were very similar to those obtained in cut slices. Although our present results suggest an important role for $GABA_A$ receptors in coupling regional oscillators, we cannot exclude the possibility that other receptors, neurotransmitters, and peptidergic signals may contribute to this interplay.

In an attempt to understand the mechanism by which GABA couples dorsal and ventral regions, we applied bicuculline pulses to the slice preparation. The results

revealed large differences in the acute responses to bicuculline of the dorsal and ventral SCN, suggesting that endogenous GABA has inhibitory effects in the ventral SCN but elicits excitatory responses in the dorsal SCN. Other studies have shown potential excitatory actions of GABA in the SCN, but there is no agreement on the presence or timing of the excitatory effects [30, 31, 39–44]. These inconsistencies may be explainable by different recording locations within the SCN. Exogenous application of GABA did not reveal spatial or temporal differences [45, 46], but these studies did not test endogeneous GABAergic activity. Measurement of postsynaptic currents in the dorsal SCN revealed a circadian rhythm in the frequency of spontaneous $GABA_A$-mediated synaptic events [47]. The use of whole-cell patch-clamp recordings, however, did not allow distinguishing between inhibitory and excitatory action of GABA because the chloride equilibrium potential was clamped. We consider that our results are indicative of intrinsic differences in responsiveness of dorsal and ventral SCN neurons to endogenous GABA. In vivo, afferent pathways such as those from the intergeniculate leaflet (IGL) or raphe nuclei are likely to contribute to the magnitude of the bicuculline response.

The induction of a secondary electrical-activity component in the dorsal part of the intact SCN is consistent with our finding that GABA excites dorsal SCN neurons. It is also consistent with the presence of a direct and dense connection from ventral to dorsal SCN, as shown in pseudorabies virus (PRV) or horseradish-peroxidase (HRP)-tracing studies and confocal fluorescence microscopy [48, 49]. Via this pathway, the ventral SCN can shift the dorsal SCN and cause it to resynchronize to the new phase. In turn, the dorsal SCN may have a weak phase-shifting effect because the initial overshoot in phase of the ventral SCN was compensated during the resynchronization period. The precise mechanism and pathway by which the dorsal SCN affects the ventral SCN remains to be clarified.

Conclusions

The present study shows that, within the rat SCN, GABAergic transmission is critically involved in communication between two groups of oscillators that differ with respect to their localization and their phase-resetting properties. What we presently know about the interregional entrainment pathways can be summarized as follows: (1) The ventral SCN receives dense retinal input [8]; (2) the ventral SCN shows light-induced gene expression [16–18]; (3) the ventral SCN resets more quickly in response to a shifted light schedule than the dorsal SCN, in both gene expression and electrical activity (see [13]; this study); (4) the ventral SCN has a strong phase-shifting effect on the dorsal SCN (see [13]; this study); (5) bicuculline application prevents transmission of phase information between dorsal and ventral SCN, indicating a critical role for $GABA_A$ in synchronizing regional oscillators (see this study); and (6) GABA can act excitatory to the dorsal SCN, and it inhibits the ventral SCN (see this study).

Collectively, these observations lead us to propose the following model (Figure 4B): For synchronization by light, only the oscillators of the ventral SCN are shifted directly by environmental cycles. Other regions of the SCN rely on interoscillator coupling for entrainment. Two forms of excitatory input are involved in synchronizing the SCN. First, the ventral SCN is shifted by light through the excitatory action of glutamate. Once shifted, the ventral SCN acts to shift the dorsal SCN via the excitatory action of GABA. The coupling between dorsal and ventral SCN is asymmetrical in that the ventral region exerts a greater effect on the final phase of the SCN than does the dorsal region. The asymmetry may be due to the different action of GABA in the dorsal and ventral regions. This is a novel and testable hypothesis, in which GABA regulates oscillator phase through excitatory rather than inhibitory action.

Experimental Procedures

Animals and Behavioral Activity

Male wild-type Wistar rats (Harlan, Horst, the Netherlands) were entrained to a 12:12 light-dark cycle. The animals were kept in cages that were equipped with a running wheel. Wheel running activity was measured every minute. Food and water were available ad libitum. After entrainment, the light-dark regime was delayed 6 hr by delaying the time of lights-off [50], which was followed by one shifted light-dark cycle (see Figure S1A). Subsequently, the animals were placed in constant darkness. All experiments were carried out under the approval of the Animal Experiments Committee of the Leiden University Medical Center.

Analysis of Behavioral-Activity Rhythms

Onsets and offsets of drinking behavior of 14 rats were scored by eye on the last day before the shift of the light-dark cycle and for 7 days in constant darkness after the shift. Wheel running-activity rhythms were measured in a separate group of animals and showed similar phase-shifting results (M.J.V. and J.H.M., unpublished data). The duration of drinking activity (α) was defined as the time between the activity onset and offset and was determined per day. The phase shifts in activity onset and offset and changes in α were investigated with ANOVA with post-hoc Dunnetts tests ($p < 0.05$).

In Vitro Electrophysiology

Brains were prepared: (1) at lights off (ZT 12), before the delay of the light-dark cycle; (2) immediately after the delay of the light-dark cycle, at the onset of constant darkness; (3) after 2 days in constant darkness; and (4) after 5 days in constant darkness (see Figure S1A). Preparation at these time points resulted in data for unshifted control slices [12] (average peak time at ZT 6.1 ± 0.7, n = 12 recordings of 6 animals) and for days 1, 3, and 6 after the delay. Additional control experiments indicated that preparation of SCN slices at the time that light induces maximum phase delays does not induce bimodal peaks or phase delays (average peak time ZT 5.3 ± 0.5, n = 6).

Multiunit electrical activity from the SCN was recorded as described previously [51]. Coronal hypothalamic slices (500 μm thick, 3.5 × 4 mm) that contained the SCN were sectioned and transferred to an interface chamber. Slices were oxygenated with humidified 95% O_2/5% CO_2 and perfused with artificial cerebrospinal fluid (ACSF) at 35°C. We used one slice per animal and attempted simultaneous recordings of multiunit neuronal activity from the dorsal and the ventral SCN with two stationary electrodes. No correlation existed between the distance from the electrode to the midline of the SCN and the incidence of bimodal peaks ($R = 0.53$, $p > 0.4$), indicating that electrical signals are only measured from neurons in close vicinity to the electrode tip.

In a second series of experiments, brain slices were prepared immediately after the delay of the light-dark cycle, and a cut was made between the dorsal and ventral SCN with a custom-made knife to completely separate these two regions bilaterally. We aimed to record multiunit activity from the separated dorsal and ventral SCN simultaneously. We measured the fraction of the dorsal

and ventral SCN as a percentage of the maximum height of the SCN. These experiments were also performed (1) immediately after a 6 hr phase advance of the light-dark cycle and (2) in slices taken from animals that did not experience a phase shift. In all cases, slices were prepared immediately after lights-off (see Figures S1B and S1C).

In a third series of experiments, intact slices were recorded on day 1 after the delay. During recording, the $GABA_A$ receptor antagonist (-)-bicuculline methochloride (Tocris Cookson, Avonmouth, Bristol, UK) was added to the perfusion medium in a concentration of 20 μM, starting several hours after slice preparation and lasting for at least 20 hr. The concentration of bicuculline was based on dosages previously used in SCN slices [31, 39, 40, 42, 44] to block $GABA_A$-mediated synaptic activity.

The final set of experiments tested the response to short applications (30 min) of bicuculline (20 μM) to intact or cut slices. Slices were prepared at lights-on (ZT 0) from animals in an unshifted light-dark regime, and the blocker was applied during the first day at ZT 3, 9, 12, 15, 21, and 0 and at ZT 3 on the second day.

Analysis of In Vitro Electrophysiology

The times of the peaks, troughs, and half-maximum values of neuronal activity were determined after the data were smoothed [52]. Because our analysis was aimed at investigating differences between the dorsal and ventral SCN, the two recordings from one slice were analyzed separately. For estimation of peak times in the first series of experiments, data from dorsal and ventral SCN were pooled.

Differences between the experimental groups (recorded on days 1, 3, and 6 after the delay) and the control group (recorded on day –1 before the delay) were tested for statistical significance via ANOVAs with post-hoc Dunnetts tests ($p < 0.05$). Each group contains data of at least six slices. The difference between the peak times of the two components of bimodal peaks, as well as differences between the peak widths, phases of peaks, troughs, and the half-maximum values of the rising and declining slopes obtained in the ventral and dorsal parts of the intact and cut SCN, was tested for statistical significance with independent t tests ($p < 0.05$). Peak width of the electrical-activity rhythm was determined by using the half-maximum values of the first rising slope and the last falling slope within one cycle. For bimodal patterns, this included both components. To determine the correlation of peak width with the duration of the behavioral activity, we pooled the data of unimodal and bimodal peaks. Data were normalized for the figures to allow visual comparison between experiments. To normalize the data, we used the maximum of the smoothed dataset and equaled this value to one.

For the analysis of the effect of short applications of bicuculline, the trend in the data was removed by linear regression. For each treatment, up to 60 min of baseline preceding the pulse was used for the regression, and the resulting line was subtracted from a 2.5 hr data segment including the pulse. Subsequently, the data were smoothed (low-pass box filter), and the maximum response during the bicuculline application was determined. A response was considered significant if it was larger than 2× the standard deviation of the baseline before smoothing. The amplitude of the responses was normalized with the average multiunit activity of the whole recording period. The differences in the magnitudes of the responses between the dorsal and ventral SCN were analyzed with independent t tests.

Supplemental Data

Supplemental Results and several supplemental figures are available at http://www.current-biology.com/cgi/content/full/15/10/886/DC1/.

Acknowledgments

We would like to thank Hans Duindam for excellent technical assistance. Research was supported by National Institutes of Health grant MH62517 to G.D.B. and by Leids Universitair Medisch Centrum Excellent Student trajectory to M.J.V.

Received: January 12, 2005
Revised: March 10, 2005
Accepted: March 29, 2005
Published: May 24, 2005

References

1. Takahashi, J.S., Turek, F.W., and Moore, R.Y. (2001). Handbook of Behavioral Neurobiology, *12*, Circadian Clocks (New York: Kluwer Academic/Plenum Publishers).
2. Reppert, S.M., and Weaver, D.R. (2002). Coordination of circadian timing in mammals. Nature *418*, 935–941.
3. Welsh, D.K., Logothetis, D.E., Meister, M., and Reppert, S.M. (1995). Individual neurons dissociated from rat suprachiasmatic nucleus express independently phased circadian firing rhythms. Neuron *14*, 697–706.
4. Yamaguchi, S., Isejima, H., Matsuo, T., Okura, R., Yagita, K., Kobayashi, M., and Okamura, H. (2003). Synchronization of cellular clocks in the suprachiasmatic nucleus. Science *302*, 1408–1412.
5. Quintero, J.E., Kuhlman, S.J., and McMahon, D.G. (2003). The biological clock nucleus: A multiphasic oscillator network regulated by light. J. Neurosci. *23*, 8070–8076.
6. Schaap, J., Albus, H., van der Leest, H.T., Eilers, P.H.C., Détári, L., and Meijer, J.H. (2003). Heterogeneity of rhythmic suprachiasmatic nucleus neurons: Implications for circadian waveform and photoperiodic encoding. Proc. Natl. Acad. Sci. USA *100*, 15994–15999.
7. Herzog, E.D., Aton, S.J., Numano, R., Sakaki, Y., and Tei, H. (2004). Temporal precision in the mammalian circadian system: A reliable clock from less reliable neurons. J. Biol. Rhythms *19*, 35–46.
8. Moore, R.Y., and Lenn, N.J. (1972). A retinohypothalamic projection in the rat. J. Comp. Neurol. *146*, 1–14.
9. Van Gelder, R.N. (2003). Making (a) sense of non-visual ocular photoreception. Trends Neurosci. *26*, 458–461.
10. Pittendrigh, C.S. (1960). Circadian rhythms and the circadian organization of living systems. Cold Spring Harb. Symp. Quant. Biol. *25*, 159–184.
11. Reddy, A.B., Field, M.D., Maywood, E.S., and Hastings, M.H. (2002). Differential resynchronisation of circadian clock gene expression within the suprachiasmatic nuclei of mice subjected to experimental jet lag. J. Neurosci. *22*, 7326–7330.
12. Vansteensel, M.J., Yamazaki, S., Albus, H., Deboer, T., Block, G.D., and Meijer, J.H. (2003). Dissociation between circadian *Per1* and neuronal and behavioral rhythms following a shifted environmental cycle. Curr. Biol. *13*, 1538–1542.
13. Nagano, M., Adachi, A., Nakahama, K., Nakamura, T., Tamada, M., Meyer-Bernstein, E., Sehgal, A., and Shigeyoshi, Y. (2003). An abrupt shift in the day/night cycle causes desynchrony in the mammalian circadian center. J. Neurosci. *23*, 6141–6151.
14. Van den Pol, A.N. (1980). The hypothalamic suprachiasmatic nucleus of rat: Intrinsic anatomy. J. Comp. Neurol. *191*, 661–702.
15. Moore, R.Y., and Silver, R. (1998). Suprachiasmatic nucleus organization. Chronobiol. Int. *15*, 475–487.
16. Yan, L., Takekida, S., Shigeyoshi, Y., and Okamura, H. (1999). *Per1* and *Per2* gene expression in the rat suprachiasmatic nucleus: Circadian profile and the compartment-specific response to light. Neuroscience *94*, 141–150.
17. Schwartz, W.J., Carpino, A., Jr., de la Iglesia, H.O., Baler, R., Klein, D.C., Nakabeppu, Y., and Aronin, N. (2000). Differential regulation of *fos* family genes in the ventrolateral and dorsomedial subdivisions of the rat suprachiasmatic nucleus. Neuroscience *98*, 535–547.
18. Lee, H.S., Billings, H.J., and Lehman, M.N. (2003). The suprachiasmatic nucleus: A clock of multiple components. J. Biol. Rhythms *18*, 435–449.
19. Hannibal, J. (2002). Neurotransmitters of the retino-hypothalamic tract. Cell Tissue Res. *309*, 73–88.

20. Moore, R.Y., Speh, J.C., and Leak, R.K. (2002). Suprachiasmatic nucleus organization. Cell Tissue Res. *309*, 89–98.
21. Shinohara, K., Honma, S., Katsuno, Y., Abe, H., and Honma, K. (1995). Two distinct oscillators in the rat suprachiasmatic nucleus *in vitro*. Proc. Natl. Acad. Sci. USA *92*, 7396–7400.
22. Noguchi, T., Watanabe, K., Ogura, A., and Yamaoka, S. (2004). The clock in the dorsal suprachiasmatic nucleus runs faster than that in the ventral. Eur. J. Neurosci. *20*, 3199–3202.
23. De la Iglesia, H.O., Cambras, T., Schwartz, W.J., and Díez-Noguera, A. (2004). Forced desynchronization of dual circadian oscillators within the rat suprachiasmatic nucleus. Curr. Biol. *14*, 796–800.
24. Jagota, A., de la Iglesia, H.O., and Schwartz, W.J. (2000). Morning and evening circadian oscillations in the suprachiasmatic nucleus *in vitro*. Nat. Neurosci. *3*, 372–376.
25. Burgoon, P.W., Lindberg, P.T., and Gillette, M.U. (2004). Different patterns of circadian oscillation in the suprachiasmatic nucleus of hamster, mouse, and rat. J. Comp. Physiol. [A] *190*, 167–171.
26. Honma, S., Shirakawa, T., Nakamura, W., and Honma, K. (2000). Synaptic communication of cellular oscillations in the rat suprachiasmatic neurons. Neurosci. Lett. *294*, 113–116.
27. Jiang, Z.G., Yang, Y.Q., and Allen, C.N. (1997). Tracer and electrical coupling of rat suprachiasmatic nucleus neurons. Neuroscience *77*, 1059–1066.
28. Colwell, C.S. (2000). Rhythmic coupling among cells in the suprachiasmatic nucleus. J. Neurobiol. *43*, 379–388.
29. Long, M.A., Jutras, M.J., Connnors, B.W., and Burwell, R.D. (2005). Electrical synapses coordinate activity in the suprachiasmatic nucleus. Nat. Neurosci. *8*, 61–66.
30. Liu, C., and Reppert, S.M. (2000). GABA synchronizes clock cells within the suprachiasmatic circadian clock. Neuron *25*, 123–128.
31. Shirakawa, T., Honma, S., Katsuno, Y., Oguchi, H., and Honma, K. (2000). Synchronization of circadian firing rhythms in cultured rat suprachiasmatic neurons. Eur. J. Neurosci. *12*, 2833–2838.
32. Michel, S., and Colwell, C.S. (2001). Cellular communication and coupling within the suprachiasmatic nucleus. Chronobiol. Int. *18*, 579–600.
33. Kim, Y.I., and Dudek, F.E. (1992). Intracellular electrophysiological study of suprachiasmatic nucleus neurons in rodents: Inhibitory synaptic mechanisms. J. Physiol. *458*, 247–260.
34. Jiang, Z.G., Yang, Y., Liu, Z.P., and Allen, C.N. (1997). Membrane properties and synaptic inputs of suprachiasmatic nucleus neurons in rat brain slices. J. Physiol. *499*, 141–159.
35. Ralph, M.R., and Menaker, M. (1989). GABA regulation of circadian responses to light. I. Involvement of $GABA_A$-benzodiazepine and $GABA_B$ receptors. J. Neurosci. *9*, 2858–2865.
36. Huhman, K.L., Babagbemi, T.O., and Albers, H.E. (1995). Bicuculline blocks neuropeptide Y-induced phase advances when microinjected in the suprachiasmatic nucleus of Syrian hamsters. Brain Res. *675*, 333–336.
37. Gillespie, C.F., Huhman, K.L., Babagbemi, T.O., and Albers, H.E. (1996). Bicuculline increases and muscimol reduces the phase-delaying effects of light and VIP/PHI/GRP in the suprachiasmatic region. J. Biol. Rhythms *11*, 137–144.
38. Gillespie, C.F., Mintz, E.M., Marvel, C.L., Huhman, K.L., and Albers, H.E. (1997). $GABA_A$ and $GABA_B$ agonists and antagonists alter the phase-shifting effects of light when microinjected into the suprachiasmatic region. Brain Res. *759*, 181–189.
39. Wagner, S., Castel, M., Gainer, H., and Yarom, Y. (1997). GABA in the mammalian suprachiasmatic nucleus and its role in diurnal rhythmicity. Nature *387*, 598–603.
40. Gribkoff, V.K., Pieschl, R.L., Wisialowski, T.A., Park, W.K., Strecker, G.J., de Jeu, M.T.G., Pennartz, C.M.A., and Dudek, F.E. (1999). A reexamination of the role of GABA in the mammalian suprachiasmatic nucleus. J. Biol. Rhythms *14*, 126–130.
41. Wagner, S., Sagiv, N., and Yarom, Y. (2001). GABA-induced current and circadian regulation of chloride in neurones of the rat suprachiasmatic nucleus. J. Physiol. *537*, 853–869.
42. De Jeu, M., and Pennartz, C. (2002). Circadian modulation of GABA function in the rat suprachiasmatic nucleus: Excitatory effects during the night phase. J. Neurophysiol. *87*, 834–844.
43. Shimura, M., Akaike, N., and Harata, N. (2002). Circadian rhythm in intracellular Cl^- activity of acutely dissociated neurons of suprachiasmatic nucleus. Am. J. Physiol. *282*, C366–C373.
44. Gribkoff, V.K., Pieschl, R.L., and Dudek, F.E. (2003). GABA receptor-mediated inhibition of neuronal activity in rat SCN in vitro: Pharmacology and influence of circadian phase. J. Neurophysiol. *90*, 1438–1448.
45. Mason, R. (1986). Circadian variation in sensitivity of suprachiasmatic and lateral geniculate neurones to 5-hydroxytryptamine in the rat. J. Physiol. *377*, 1–13.
46. Liou, S.Y., Shibata, S., Albers, H.E., and Ueki, S. (1990). Effects of GABA and anxiolytics on the single unit discharge of suprachiasmatic neurons in rat hypothalamic slices. Brain Res. Bull. *25*, 103–107.
47. Itri, J., Michel, S., Waschek, J.A., and Colwell, C.S. (2004). Circadian rhythm in inhibitory synaptic transmission in the mouse suprachiasmatic nucleus. J. Neurophysiol. *92*, 311–319.
48. Leak, R.K., Card, J.P., and Moore, R.Y. (1999). Suprachiasmatic pacemaker organization analyzed by viral transynaptic transport. Brain Res. *819*, 23–32.
49. Romijn, H.J., Sluiter, A.A., Pool, C.W., Wortel, J., and Buijs, R.M. (1997). Evidence from confocal fluorescence microscopy for a dense, reciprocal innervation between AVP-, somatostatin-, VIP/PHI-, GRP- and VIP/PHI/GRP-immunoreactive neurons in the rat suprachiasmatic nucleus. Eur. J. Neurosci. *9*, 2613–2623.
50. Yamazaki, S., Numano, R., Abe, M., Hida, A., Takahashi, R., Ueda, M., Block, G.D., Sakaki, Y., Menaker, M., and Tei, H. (2000). Resetting central and peripheral circadian oscillators in transgenic rats. Science *288*, 682–685.
51. Albus, H., Bonnefont, X., Chaves, I., Yasui, A., Doczy, J., van der Horst, G.T.J., and Meijer, J.H. (2002). Cryptochrome-deficient mice lack circadian electrical activity in the suprachiasmatic nuclei. Curr. Biol. *12*, 1130–1133.
52. Schaap, J., Albus, H., Eilers, P.H.C., Détári, L., and Meijer, J.H. (2001). Phase differences in electrical discharge rhythms between neuronal populations of the left and right suprachiasmatic nuclei. Neuroscience *108*, 359–363.